

# Structure-based design and in flow synthesis of aromatic endoperoxides acting as oxygen releasing agents

Marco Agnes,<sup>\*a</sup> Adelaide Santagata,<sup>a</sup> Daniele Veclani,<sup>a</sup> Alessandro Venturini,<sup>a</sup> Magda Monari,<sup>b</sup> Paolo Dambruoso,<sup>a</sup> and Ilse Manet<sup>\*a</sup>

<sup>a</sup> *Istituto per la Sintesi Organica e la Fotoreattività (ISOF), Consiglio Nazionale delle Ricerche (CNR) - Via Gobetti 101, 40129 Bologna, Italy*

<sup>b</sup> *Dipartimento di Chimica "Giacomo Ciamician", Alma Mater Studiorum – Università di Bologna - Via P. Gobetti 85, 40129, Bologna, Italy*

*\* Corresponding authors:*

[marco.agnes@isof.cnr.it](mailto:marco.agnes@isof.cnr.it) - [ilse.manet@isof.cnr.it](mailto:ilse.manet@isof.cnr.it)

## Graphical Abstract

### Relieving hypoxia in solid cancer



Structural insights from computational and crystallographic analysis of an array of aromatic substrates supported the design and synthesis of three novel endoperoxides of 9,10-disubstituted anthracene derivatives with promising ability to reversibly bind molecular oxygen and release it in biocompatible conditions with the aim to relieve hypoxic conditions in hazardous diseases.

## Abstract

Hypoxia occurs in different pathological settings as a consequence of poor vascularization and it results in reduced efficacy of some current nosocomial treatments i.e. chemotherapy and photodynamic therapy. In order to overcome these boundaries, aromatic endoperoxides (EPOs) have been studied and proposed as oxygen-releasing agents (ORAs) due to their ability to reversibly bind molecular oxygen (O<sub>2</sub>), liberating it upon suitable triggering. DFT calculation of the dissociation energy ( $E_{\text{diss}}$ ) of the intramolecular O-O bridge and structural crystallographic data of synthesized and studied EPOs drove the design of an array of 9,10-disubstituted anthracenes among which three candidates were carefully selected. Once optimized the synthesis of the aromatic substrates, for the first time the corresponding EPOs have been produced under continuous flow irradiation in the presence of a sub-stoichiometric amount of a photosensitizer in organic solvents. The release of O<sub>2</sub> could be obtained straightforwardly at 37.5 °C by thermolysis. In accordance with the calculated  $E_{\text{diss}} = 3.2 \text{ kcal mol}^{-1}$  and an experimental  $t_{1/2} = 40$  minutes, 3,3'-(anthracene-9,10-diyl)bis(prop-2-yn-1-ol) resulted as the best candidate for the sustained release of O<sub>2</sub> under physiologically relevant conditions. Its exploitation as ORA to relieve hypoxia will be evaluated and described in due course.

## Keywords

DFT

Hypoxia

Flow chemistry

Oxygen release

Photochemistry.

## Introduction

Hypoxia is a condition occurring in several disorders resulting in lower levels (1-5%) of molecular oxygen ( $O_2$ ) compared to the normoxic conditions of healthy physiological environment, where the  $O_2$  tension is typically between 10 and 21%.<sup>[1]</sup> This status is mainly induced by the poor vascularization or impaired blood flow characterizing potentially fatal illnesses like solid tumors,<sup>[2,3]</sup> microbial<sup>[4]</sup> and fungal<sup>[5]</sup> infections and biofilms, cerebral<sup>[6]</sup> and myocardial<sup>[7]</sup> ischemia, etc. The harshness of hypoxia resides in its ability to annihilate the efficacy of current drug-based therapies as it boosts drug resistance<sup>[4]</sup> and to reduce the effects of radiotherapy<sup>[8]</sup> and photodynamic therapy (PDT)<sup>[9]</sup> as well.

In order to overcome hypoxia-related limitations, the design and development of biocompatible molecular vectors able to deliver  $O_2$  directly to the target tissues is gaining significant attention in the pharmacological field.<sup>[9]</sup> In this context, an increasing amount of literature focused on aromatic endoperoxides (EPOs) as suitable Oxygen-Releasing Agents (ORAs).<sup>[10]</sup> The polycyclic aromatic precursors are cheap, versatile substrates able to reversibly bind and release  $O_2$  when properly functionalized and stimulated. The chemistry of these interesting EPOs has been deepened in the past<sup>[11]</sup> and many aspects regarding their preparation and reactivity are now well-known and established.<sup>[12]</sup> Among others, the group of W. Fudickar and T. Linker was able to produce a remarkable amount of EPOs from both anthracene<sup>[13,14]</sup> and naphthalene<sup>[15,16]</sup> derivatives.

The addition to polycyclic aromatic precursors of singlet oxygen ( $^1O_2$ ) photochemically generated in situ upon irradiation of the reaction mixture containing a sub-stoichiometric amount of a photosensitizer (PS), is a most efficient way to form EPOs.<sup>[10]</sup> This photooxygenation reaction is straightforward and typically results in final products bearing the target intramolecular O-O bridge. Selection and positioning of the substituents on the aromatic cores are crucial for the overall ability to selectively bind and release  $O_2$ .

The smooth release of  $O_2$  either in its triplet or singlet state is usually induced by thermolysis, driving to the restoration of the parent aromatic precursors.<sup>[17]</sup> However, being these molecules studied in parallel for applications in the fields of electronic<sup>[18]</sup> and optical<sup>[19]</sup> devices, organic semiconductors<sup>[20]</sup> and printing,<sup>[21]</sup> the design of EPOs usually does not consider biocompatibility and often the temperatures needed for triggering the  $O_2$  release are above 50 °C.

In a previous work,<sup>[22]</sup> a series of anthracene or naphthalene derivatives were synthesized and tested as ORAs (Figure 1). Compared to previously published literature,<sup>[23]</sup> effective improvements were achieved in the photooxygenation of mono- and di-substituted anthracene derivatives, namely 4-(anthracen-9-yl)benzoic acid, ANBA, and 4-(10-phenylanthracen-9-yl)benzoic acid, PABA, respectively, forming more stable EPOs compared to the analogous naphthalene-derivatives, 4-(naphthalen-1-yl)benzoic acid, NABA, and 4-(4-phenylnaphthalen-1-yl)benzoic acid, PNBA. Out of four, only PABA-O<sub>2</sub> was found to release  $O_2$  effectively, when heated at 90 °C for a prolonged time.

Herein, computational and crystallographic data were used to select the most suitable structural features to improve the ORA performances in terms of EPO formation and  $O_2$  release. For the first time, the synthesis of anthracene-based EPOs bearing carefully selected substituents was carried out using a continuous flow photochemical reactor allowing to envisage the industrial scale up of the photooxygenation step (Figure S1). Importantly, as anticipated by computational insights, these EPOs release  $O_2$  in physiologically compatible conditions thus suggesting the possibility to further explore these molecules as ORAs for relieving hypoxia.

## Results and Discussion

### Computational studies

The aim of the computational analysis was to screen an array of aromatic derivatives consisting of previously published compounds taken as reference[22,24] and new proposed structures which were envisaged to have better performances as ORA at physiologically relevant conditions.

It is established that the electronic character, position and size of substituents have a direct influence on the kinetics of formation, regiochemistry and stability of aromatic EPOs.[25] In particular, considering a concerted mechanism of the [4+2] reaction between the aromatic substrates and the  $^1\text{O}_2$  generated in situ,[11] their readiness to bind and release  $\text{O}_2$  can be directly related to the dissociation energy ( $E_{\text{diss}}$ ) calculated using the density functional theory (DFT). The computed  $E_{\text{diss}}$  of the EPOs of NABA and PNBA resulted to be  $-3.49 \text{ kcal} \cdot \text{mol}^{-1}$  and  $-4.31 \text{ kcal} \cdot \text{mol}^{-1}$ , respectively, while in the case of PABA and ANBA it was found to be  $10.44 \text{ kcal} \cdot \text{mol}^{-1}$  and  $12.16 \text{ kcal} \cdot \text{mol}^{-1}$ , respectively (Figure 1, Table S2). The negative values obtained for NABA and PNBA confirmed the lack of any stabilizing effect observed experimentally as the formation of the O-O bridge could not be detected. The opposite behaviour of PABA and ANBA with large positive  $E_{\text{diss}}$  values is in line with the straightforward formation of EPOs in solution and, above all, their high stability. In fact, only heating at  $90^\circ\text{C}$  for several hours afforded the clean release of  $\text{O}_2$  from PABA- $\text{O}_2$  with similar performances in organic solvent and water, upon complexation with a polymeric matrix.[22]

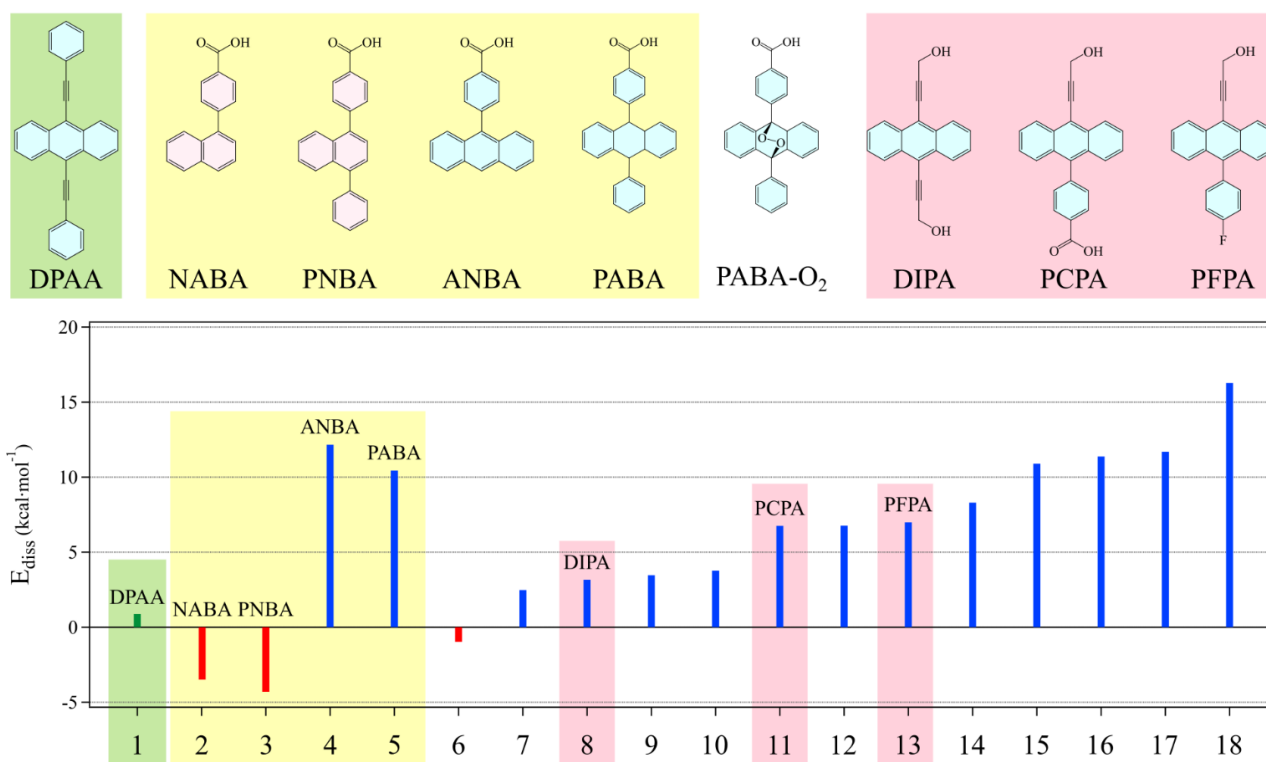


**Figure 1:** Top panel: chemical structure of reference compound (green background) 9,10-diphenylalkynylanthracene (DPAA); previously reported compounds (yellow background): 4-(anthracen-9-yl)benzoic acid, ANBA, 4-(10-phenylanthracen-9-yl)benzoic acid, PABA, 9,10-endoperoxide of PABA, PABA- $\text{O}_2$ , 4-(naphthalen-1-yl)benzoic acid, NABA, 4-(4-phenylnaphthalen-1-yl)benzoic acid, PNBA; newly synthesized compounds (pink background): 3,3'-(anthracene-9,10-diyl)bis(prop-2-yn-1-ol), DIPA, 4-(10-(3-hydroxyprop-1-yn-1-yl)anthracen-9-yl)benzoic acid, PCPA, 3-(10-(4-fluorophenyl)anthracen-9-yl)prop-2-yn-1-ol, PFPA. Bottom panel: Plot of the dissociation energies ( $E_{\text{diss}}$ , kcal mol<sup>-1</sup>) for a series of anthracene derivatives obtained by density functional theory (DFT) B3LYP/Def-TZP/dichloromethane calculations (see Table S2 for correlating the numbers to the structures).

Despite the well-known effect of electron-withdrawing (EWGs) or electron donating groups (EDGs) on the rate of formation and stability of aromatic EPOs, ANBA, PABA, NABA and PNBA decorated with the same substituents oriented perpendicular to the conjugated cores thus reducing the electronic effect, showed quite divergent calculated  $E_{\text{diss}}$ . Hence DFT analysis was further meant to verify if steric interactions could contribute to the overall binding process thanks to the use of 2D and 3D color-filled reduced gradient density (RGD) projections (Figure S3). No major differences could be found between the two sets of molecules in the intensity of VdW and steric interactions. However, the aromatic substituents on NABA and PNBA are less tilted compared to the anthracene analogues, lowering the possibilities to establish any interaction and thus resulting in the impossibility to observe such EPOs experimentally.

In light of these results, the focus of the predictive analysis was narrowed to the anthracene-based EPOs, seeking for substrates displaying  $E_{\text{diss}} < 10 \text{ kcal mol}^{-1}$ . 9,10-diphenylalkynylanthracene (DPAA) has been reported to have a half-life ( $t_{1/2}$ ) of 23 minutes at 25 °C in toluene.[25] Being this value closer to our goal of sustained release of  $\text{O}_2$  at 37.5°C, its calculated  $E_{\text{diss}} = 0.88 \text{ kcal} \cdot \text{mol}^{-1}$  was taken as lower limit. Moreover, considering the application as therapeutic agents, fully hydrophobic molecules were not taken into consideration, while the presence of hydroxylic, carboxylic and more hydrophilic functional groups was preferred in order to boost their water solubility and/or allow further functionalization. A total of 13 anthracene structures bearing different combination of EDGs or EWGs were tested and compared with DPAA, PABA and ANBA (Table S2).

Among the newly designed molecules (entries 6-18 in Table S2), structure 6, bearing a tris-trifluoromethyl-benzene at position 9 and a prop-2-yn-1-ol moiety at position 10 showed a negative  $E_{\text{diss}}$  value =  $-0.98 \text{ kcal mol}^{-1}$  (Figure 1) induced by unfavourable steric effects (Figure S4) and it was not further considered. Structures 7 to 10, bearing the prop-2-yn-1-ol group(s) in position 9 and/or 10, showed interesting  $E_{\text{diss}}$  ranging from 2.47 to 3.77  $\text{kcal} \cdot \text{mol}^{-1}$ , expected to have a slightly higher stability compared to DPAA. Structures 11 to 14 exhibited remarkable  $E_{\text{diss}}$  between 6.75 and 8.30  $\text{kcal} \cdot \text{mol}^{-1}$ , while structures 15 to 18 displayed  $E_{\text{diss}} > 10.89 \text{ kcal} \cdot \text{mol}^{-1}$  thus they were not further considered.

Eventually, three molecules, 8, 11 and 13, were selected to be synthesized as suitable ORA candidates, namely:

8. 3,3'-(anthracene-9,10-diyl)bis(prop-2-yn-1-ol), DIPA ( $E_{\text{diss}} = 3.16 \text{ kcal mol}^{-1}$ )
11. 4-(10-(3-hydroxyprop-1-yn-1-yl)anthracen-9-yl)benzoic acid, PCPA ( $E_{\text{diss}} = 6.75 \text{ kcal mol}^{-1}$ )
13. 3-(10-(4-fluorophenyl)anthracen-9-yl)prop-2-yn-1-ol, PFPA ( $E_{\text{diss}} = 6.98 \text{ kcal mol}^{-1}$ )

Symmetrical DIPA, bearing prop-2-yn-1-ol moieties in positions 9 and 10 is expected to release  $\text{O}_2$  at low temperature and to be more suitable for further functionalization and increased water solubility thanks to the terminal hydroxyl groups. Unsymmetrical PCPA and PFPA, bearing a prop-2-yn-1-ol moiety in position 9 and a para benzoic acid or a para fluorophenyl group, respectively, in position 10, were supposed to generate EPOs more stable than DIPA, but more labile than PABA. The different ionisable and non ionisable appendages may be an interesting feature to regulate their solubility and further covalent or non-covalent manipulation.

### X-ray crystallographic analysis

Single crystal analysis identified structural, distinctive features for anthracene and naphthalene derivatives regarding the relative position of the aromatic cores and substituents (Figure 2).

ANBA and PABA crystallized with a single molecule per asymmetric unit and almost orthogonal dihedral angles between the anthracene plane and the aromatic substituents:  $82.84(4)^\circ$  for ANBA;  $87.5$  and  $83.1(2)^\circ$  for PABA (Figure 2a). PFPA crystallized with two molecules per asymmetric unit and the aromatic substituent is oriented at  $77.2(1)^\circ$  with respect to the anthracene plane. One O–H...O hydrogen bond links together the two conformers present in the asymmetric unit and a non-classical intermolecular H bond (C–H...F) was observed (Figure S5). PABA-O2 showed loss of planarity in the central ring of the anthracene unit due to the formation of the O–O bond with the C atoms bound to the substituents that, instead, maintain their orientation (Figure 2c). Moreover, its crystalline and calculated structures overlap significantly, suggesting no major differences between the conformation of the EPO as a solid and in solution.

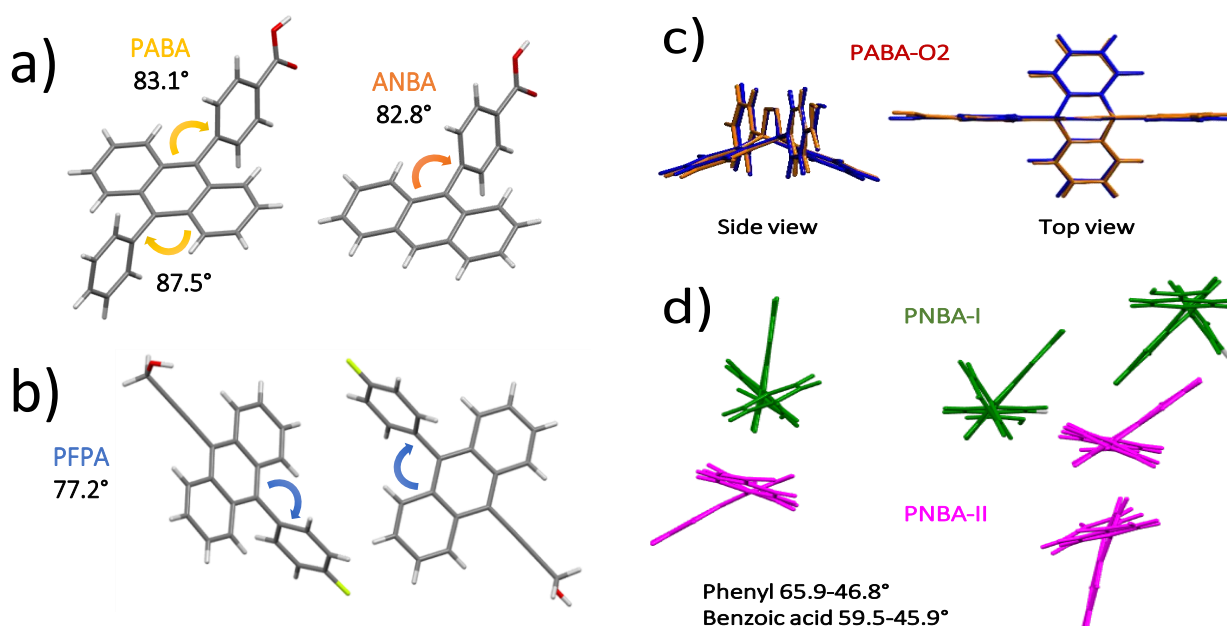


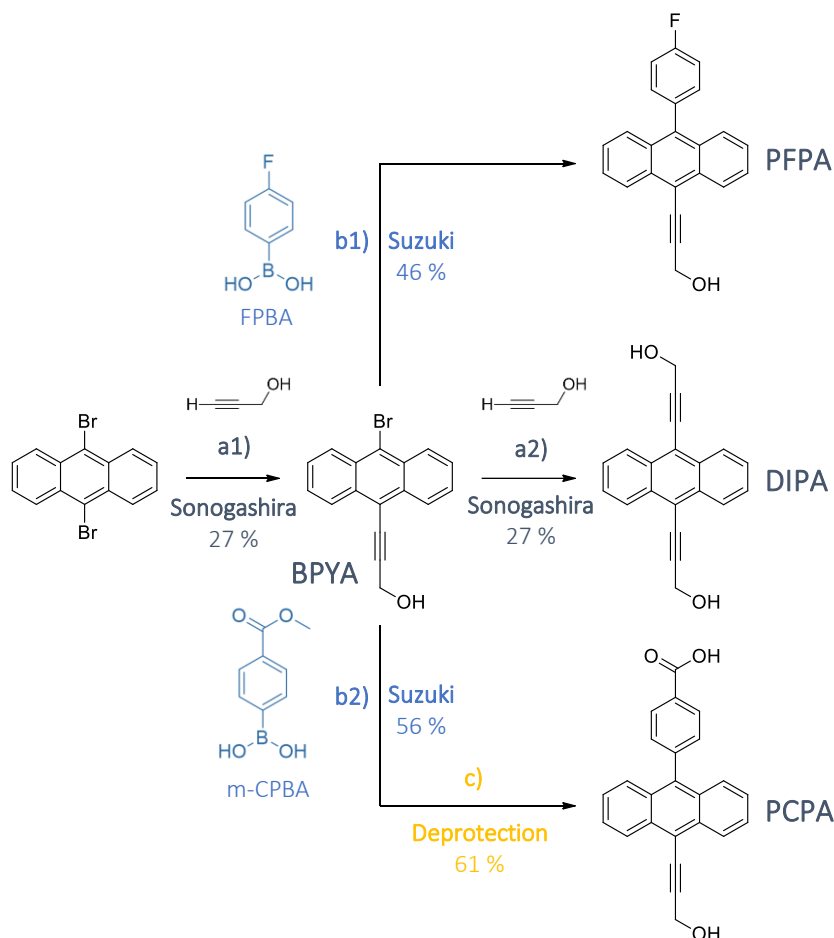
**Figure 2:** a) Crystal structures of **PABA** and **ANBA**. b) Asymmetric unit of **PFPA** crystals. c) Superimposed calculated (blue) and crystalline (orange) structures of **PABA-O2**. d) Asymmetric unit of **PNBA** crystals, composed of six different molecules, divided into two subgroups according to the different angle between substituents: PNBA-I (green structures):  $65.1 - 75.2^\circ$ , PNBA-II (magenta structures):  $17.8 - 20.2^\circ$ .

In the case of naphthalene derivatives, the crystal structure of NABA was found to match previously published data (Figure S2),<sup>[28]</sup> displaying a dihedral angle of  $46.8^\circ$ . Interestingly, PNBA crystallized adopting six different conformers (Figure 2d). The dihedral angles between the phenyl rings and the naphthalene skeleton range from  $65.85$  to  $46.75(5)^\circ$  whereas the dihedral angles between the benzoic acid rings and the naphthalene moiety range similarly from  $45.88$  to  $59.49(5)^\circ$ . In the solid state of PNBA, two distinct arrangements are present: one in which the two aromatic substituents are aligned (mutual dihedral angles from  $17.83$  to  $20.23(5)^\circ$ ) and one in which they are oriented in different directions (mutual dihedral angles from  $65.09$  to  $75.18(5)^\circ$ ) presumably to optimize packing effects.

In accordance with DFT calculations and experimental data, the relative orientation of the substituents should be more favorable for anthracene derivatives, empowering the choice of the target candidates.

### Synthesis of aromatic substrates

The synthesis of symmetrical and unsymmetrical alkynyl-bearing anthracene derivatives was achieved by Sonogashira[24,25] and Suzuki[22] couplings adapting published procedures and using 9,10-dibromoanthracene (DBA) as starting material (Scheme 1).



**Scheme 1:** Synthetic steps for the synthesis of **DIPA**, **PFPA** and **PCPA**. *Sonogashira coupling* (step a): Pd(PPh<sub>3</sub>)<sub>2</sub>Cl<sub>2</sub>, CuI, Diisopropylamine, Propargyl alcohol, THF, reflux. *Suzuki coupling* (step b): Pd(PPh<sub>3</sub>)<sub>4</sub>, CsCO<sub>3</sub> 2M<sub>(aq)</sub>, b1) (4-fluorophenyl)boronic acid (FPBA); b2) 4-(methoxycarbonyl)phenylboronic acid (m-CPBA), THF, reflux. Deprotection of methyl ester (step c): LiOH 2M<sub>(aq)</sub>, MeOH, reflux.

Formation and isolation of the mono-substituted 9-bromo-10-prop-2-yn-1-ol-anthracene (BPYA) after Sonogashira reaction in the presence of propargyl alcohol was relatively straightforward and the intermediate was obtained with a 27 % yield. In order to obtain DIPA, the same reaction was left with enough equivalents of reactants for a prolonged time in order to substitute the remaining bromine atom eventually reaching the double substitution with an overall yield of 27 %.

Different approaches were tested in order to increase the yields of the final step:

- Two-step reaction, repeating the same procedure on isolated BPYA
- Protection of the -OH groups of the propargyl alcohol with tert-butyldimethylsilyl or trimethylsilyl groups
- Reduction of the amount of Cu<sup>2+</sup> catalyst known to favor cross-coupling between alkynyl terminal moieties
- The use of organic bases others than di-isopropylamine, i.e. triethylamine.



None of the proposed changes led to significant improvements in the yield of the reaction (data not shown).

In order to synthesize PFPA and PCPA, the intermediate BPYA underwent Suzuki reactions with 4-fluorophenyl-boronic acid (FPBA) and 4-(methoxycarbonyl)phenylboronic acid (m-CPBA), respectively (Scheme 1). PFPA was isolated directly after column chromatography with a 46 % yield, while the methyl-protected intermediate obtained in a 56 % yield was treated with LiOH to eventually obtain the final product PCPA with a 61 % yield. Detailed description of the synthetic procedures and full NMR and MS characterization of the products are shown in the SI.

### Photooxygenation step in flow

The synthesis of aromatic EPOs has been optimized adapting a previously published procedure[22] to a photochemical reactor equipped for continuous flow irradiation (Vapourtec® E-Series, see SI for detailed description of the instrument and the synthetic procedure). The interest of the synthetic organic community towards flow processes is rapidly growing for an increasing number of applied chemical processes.[29] In particular, photo-induced and catalyzed transformations capitalized on the use of this technology to improve reaction rate, yield and batch size, especially thanks to the massive surface-to-volume ratio enabling increased efficiency and homogeneity of irradiation.[30]

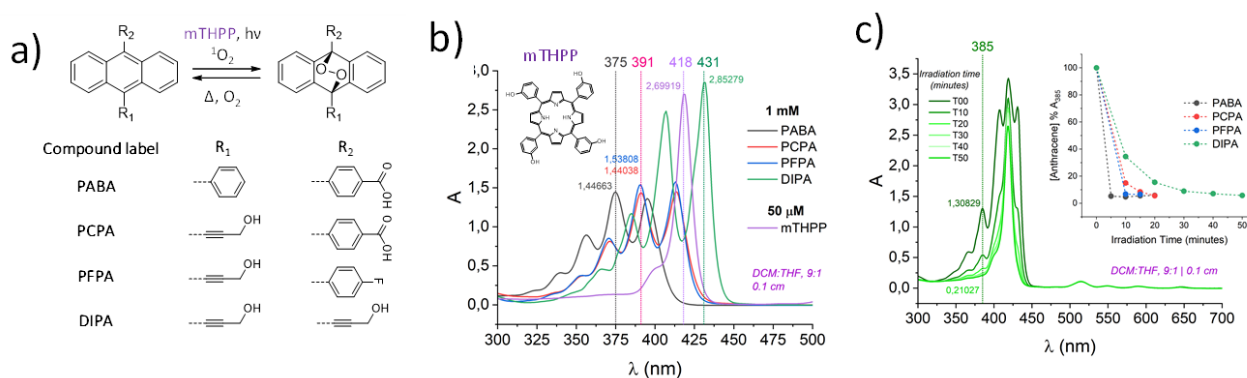


**Figure 3:** a) General scheme for the reversible binding of photosensitized  $^1O_2$  to aromatic substrates; b) UV-Vis absorption spectra (1 mM, 0.1 cm, DCM:THF 9:1) of **PABA**, **PCPA**, **PFPA** and **DIPA**; c) UV-Vis absorption spectra (0.1 cm, DCM:THF 9:1) monitoring the photosensitized synthesis of EPOs starting from the aromatic substrates in the presence of 5 % mol/mol of mTHPP (1 or 2 mL/minute *in flow* irradiation with a 525 nm LED, residence time: 10 or 5 minutes,  $T_{set} = 0$  or 25 °C).

For our purpose, the reactor was endowed with a LED lamp emitting at 525 nm ( $\pm 10$  nm) and it enabled fine control of the light intensity, the inner reactor temperature and the flow rate, which could be adjusted according to the desired residence time.

First of all, the stability of the PS was tested in DCM:THF, 9:1 (Figure S6). The readily available methylene blue, MB, despite its low absorption at the selected wavelength ( $\epsilon_{525} \approx 4000 \text{ M}^{-1} \cdot \text{cm}^{-1}$ ) entirely bleached upon irradiation, while 5, 10, 15, 20-tetrakis(3-hydroxyphenyl)-porphyrin (mTHPP,  $\epsilon_{525} = 10000 \text{ M}^{-1} \cdot \text{cm}^{-1}$ ) was photostable under the same conditions. PABA was exploited as reference substrate for the photooxygenation step being its EPO analogue PABA-O<sub>2</sub> readily formed and easy to handle (Figure 3a). Various combinations of residence times, light intensities and molar ratios between PABA and PS (either MB or mTHPP) were tested in order to optimize the *in flow* reaction conditions with respect to the previously published procedure based on a 100 W Hg-lamp setup (Figures S7, S8). Eventually, the performance of the photochemical step in flow yielded quantitative formation of PABA-O<sub>2</sub> reducing 5 times the amount of PS (1% mol/mol) in only 10 minutes, resulting in a 6-fold faster reaction compared to previously reported batch conditions.[22] Moreover, the same performance was achieved by using 80% of the intensity of irradiating light enabling even milder reaction conditions.



All the tested anthracenes showed similar absorption profiles and their molar absorption coefficients ( $\epsilon$ ,  $M^{-1} \text{ cm}^{-1}$ ) were found in the range  $15000 \pm 1500$  for PABA, PFPA and PCPA, and about 28000 for DIPA (Figure 3b). Interestingly, shifting from two aromatic substituents (PABA,  $A_{\text{max}} = 375 \text{ nm}$ ) to one aromatic and one alkynyl group (PCPA, PFPA,  $A_{\text{max}} = 391 \text{ nm}$ ) and lastly to the two alkynyl groups (DIPA  $A_{\text{max}} = 431 \text{ nm}$ ), a bathochromic shift was observed in the absorption spectra, reflecting the effect of the extended conjugation on the aromaticity of these compounds.

The reaction monitoring could be achieved by UV-Vis absorption spectroscopy following the disappearing of the absorption bands of the aromatic substrates upon formation of the EPOs (Figure 3c). Since the formation of the O-O bridge breaks the aromaticity of the central ring of the anthracenes, their characteristic absorption bands in the region between 325 and 450 nm decrease proportionally to the reaction extent. Upon exclusive, quantitative formation of the target EPOs, the final absorption spectra showed only the profile of the PS above 300 nm.

The newly synthesized aromatic substrates PFPA, PCPA and DIPA were quantitatively converted to the corresponding EPOs PFPA-O<sub>2</sub>, PCPA-O<sub>2</sub> and DIPA-O<sub>2</sub> (Figures S9, S10, S11, S12) using the following parameters:

- 5 % mol/mol of PS compared to the aromatic substrate
- 100 % of intensity of LED lamp emitting at 525 nm
- Flow rate: 0.5, 1 or 2 mL min<sup>-1</sup>
- 5 to 20 minutes of residence time
- $T_{\text{set}} = 25 \text{ }^\circ\text{C}$  for all anthracenes except for DIPA, whose corresponding EPO was reverting at room temperature so fast that it required to be irradiated at  $T_{\text{set}} = 0 \text{ }^\circ\text{C}$ .

Under the set conditions, it was possible to quantitatively convert 1  $\mu\text{mol}/\text{min}$  (corresponding on average to about 0.4 mg/min) of substrate to EPO.

#### *Cycloreversion upon thermolysis: kinetic of O<sub>2</sub> release*

Purification and isolation of the pure EPOs could not be achieved due to the thermal instability of the molecules. However, considering the low amount of PS (5% mol/mol) and quantitative conversion of the parent substrates, cycloreversion of the EPOs was investigated on the reaction crudes once concentrated to dryness with the use of a Smart Evaporator<sup>®</sup> working at room temperature under vacuum. The obtained solid residues could be stored at  $-18^\circ\text{C}$  up to ten days. Despite also DIPA-O<sub>2</sub> was found to be stable in the reaction mixture at  $-18 \text{ }^\circ\text{C}$  for over one week (Figure S13), the compound resulted to revert to DIPA during solvent removal.

Cycloreversion of EPOs to their corresponding parent compounds was monitored in DMSO using (Figure 4):

- UV-Vis: to evaluate the kinetics of O<sub>2</sub> release at different temperatures (Figures S9, S10, S11, S12)
- <sup>1</sup>H-NMR: to qualitatively confirm the formation of the parent compounds proving the reversibility of the reaction and the lack of side processes (Figures S15, S16, S17).

UV-Vis monitoring was performed over a period of 75 minutes at different set temperatures: 25, 37.5, 45 and 50  $^\circ\text{C}$ . At 25  $^\circ\text{C}$ , only DIPA-O<sub>2</sub> was found to partially start the conversion, while at 45 and 50  $^\circ\text{C}$  all the newly synthesized EPOs were found to significantly release O<sub>2</sub>. At physiologically relevant

temperature, 37.5 °C (Figure 4a), detectable amount of parent compounds PFPA and PCPA could be observed while PABA-O2 did not show any release. However, DIPA-O2 outperformed the other candidates showing nearly quantitative conversion to parent DIPA in 75 minutes.

Accordingly, the <sup>1</sup>H NMR spectra acquired over time of PCPA-O2, PFPA-O2 and DIPA-O2 stored at 50 °C, showed full recovery of DIPA within < 0.5 h and > 75 % recovery of PFPA and PCPA after 35 h. Moreover, the lack of signals related to potential impurities confirmed that the cycloreversion reaction was the only process happening upon thermolysis.

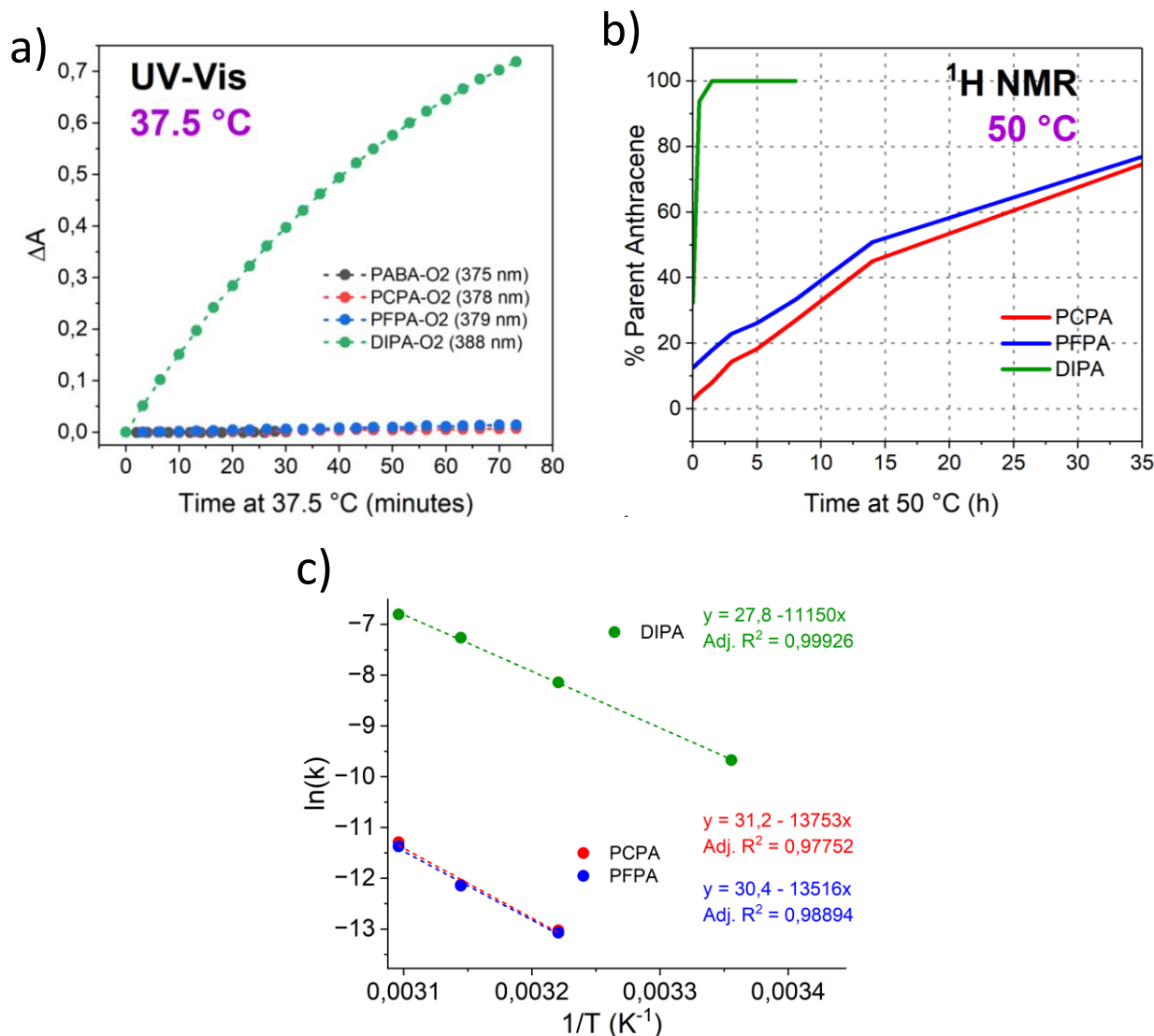


**Figure 4:** O<sub>2</sub> release monitoring by a) UV-Vis at 37.5 °C (DMSO, ΔA = difference between the starting A value and the experimental ones over time); b) <sup>1</sup>H NMR (500 MHz, DMSO-*d*<sub>6</sub>) of the compounds stored at 50 °C. c) Arrhenius plots from UV-Vis spectra monitoring the thermolysis of PCPA-O2, PFPA-O2 and DIPA-O2 at 37.5, 45 and 50 °C. For DIPA-O2, also data at 25 °C were included.

The UV-Vis data were used to calculate the thermolysis rate constants (*k*, s<sup>-1</sup>) as well as the half-life time (*t*<sub>1/2</sub>) of the EPOs, shown in Table 1 for 37,5°C. The Activation Energy (AE) for O<sub>2</sub> release was obtained from the Arrhenius plots for each substrate (Figures S14, Figure 4c).

**Table 1.** Rate constant (*k*, s<sup>-1</sup>) and half-life time (*t*<sub>1/2</sub>) for O<sub>2</sub> release at 37.5 °C and thermolysis activation energy (kJ/mol) obtained from UV-Vis data.

Compound	<i>k</i> (s <sup>-1</sup> )	AE (kJ mol <sup>-1</sup> )	<i>t</i> <sub>1/2</sub>
DIPA-O2	2.9 x 10 <sup>-4</sup>	93	40 min

PCPA-O2	2.2 x 10-6	114	87 h
PFPA-O2	2.1 x 10-6	113	92 h

PCPA-O2 and PFPA-O2 showed overlapping kinetic profiles eventually resulting in similar  $t_{1/2} \approx 90$  h at 37.5 °C. DIPA-O2, instead, showed AE value in line with the thermolysis occurring at room temperature (93 kJ mol<sup>-1</sup>), confirmed by the calculated  $t_{1/2} \approx 40$  minutes at 37.5 °C.

## Conclusion

This work collected most recent advances on the successful preparation of innovative systems based on aromatic endoperoxides (EPOs) to be used as oxygen-releasing agents (ORAs) in the treatment of hypoxia.

Computational DFT data afforded the dissociation energy ( $E_{\text{diss}}$ ) for a series of anthracene-derivatives to be exploited as EPOs. Starting from a set of known molecules, three anthracene derivatives were selected as suitable candidates according the calculated values of  $E_{\text{diss}}$ . DIPA, PCPA, and PFPA were prepared by addition of alkynyl and/or aromatic substituents in positions 9 and 10 of the anthracene scaffold and the crystallographic analysis of these structures confirmed the favorable orientation of the appended moieties to accommodate the EPO bridges.

The successful synthesis of the novel aromatic substrates was achieved upon optimization of Sonogashira and Suzuki couplings, while the target EPOs were prepared for the first time with the use of a continuous flow photoreactor in the presence of a sub-stoichiometric amount of photosensitizer (mTHPP).

Thermolysis of the substrates was then proven and monitored by UV-Vis and <sup>1</sup>H NMR spectroscopies for all compounds. However, while for PCPA-O2 and PFPA-O2 significant O2 release was achieved only at T > 45 °C, the best ORA candidate DIPA-O2 displayed a  $t_{1/2} \approx 40$  minutes already at 37.5 °C.

Further studies on this system are expected to afford their exploitation in physiological media and biocompatible conditions. In fact, solubilization in water with a hydrophilic carrier and in situ delivery has been proven to prevent the expected toxicity of anthracene-derivatives and simultaneously taking advantage of their therapeutic effects.[31] Moreover, for the purpose of hypoxia relieving in a combination therapy regime, both <sup>3</sup>O<sub>2</sub> and <sup>1</sup>O<sub>2</sub> could serve either as a substrate for PDT or as reactive oxygen species (ROS) itself. Eventually, considering the optical properties of anthracenes, the use of these derivatives could allow not only the treatment of hypoxia to restore the therapeutic performance of commercial drugs, but also the visualization of the readily emitting anthracene derivative for theranostic purposes.

## Supporting Information

The authors have cited additional references within the Supporting Information.

## Acknowledgements

The NextGeneration EU Programme is kindly acknowledged for supporting the Ecosystem for Sustainable Transition in Emilia-Romagna (ECOSISTER). The European Union (EU)'s Horizon Europe Research and Innovation Programme is also acknowledged for funding the Marie Skłodowska-Curie grant agreement Bicyclos N° 101130235. Views and opinions expressed are however those of the authors only and do not necessarily reflect those of the EU which cannot be held responsible for them. Open Access Funding was provided by Consiglio Nazionale delle Ricerche (CNR) within the CRUI-CARE Agreement.

## References

- [1] In *Encycl. Ref. Genomics Proteomics Mol. Med.*, Springer Berlin Heidelberg, Berlin, Heidelberg, 2006, pp. 853–853.
- [2] A. C. Gonçalves, E. Richiardone, J. Jorge, B. Polónia, C. P. R. Xavier, I. C. Salaroglio, C. Riganti, M. H. Vasconcelos, C. Corbet, A. B. Sarmento-Ribeiro, *Drug Resist. Updat.* 2021, 59, DOI 10.1016/j.drug.2021.100797.
- [3] F. Marcucci, C. Rumio, *Neoplasia (United States)* 2021, 23, 234–245.
- [4] B. Schaible, C. T. Taylor, K. Schaffer, *Antimicrob. Agents Chemother.* 2012, 56, 2114–2118.
- [5] C. H. Kowalski, K. A. Morelli, D. Schultz, C. D. Nadell, R. A. Cramer, *Proc. Natl. Acad. Sci. U. S. A.* 2020, 117, 22473–22483.
- [6] F. Adhami, G. Liao, Y. M. Morozov, A. Schloemer, V. J. Schmithorst, J. N. Lorenz, R. S. Dunn, C. V. Vorhees, M. Wills-Karp, J. L. Degen, R. J. Davis, N. Mizushima, P. Rakic, B. J. Dardzinski, S. K. Holland, F. R. Sharp, C. Y. Kuan, *Am. J. Pathol.* 2006, 169, 566–583.
- [7] G. Loor, P. T. Schumacker, *Cell Death Differ.* 2008, 15, 686–690.
- [8] W. Boulefour, E. Rowinski, S. Louati, S. Sotton, A. S. Wozny, P. Moreno-Acosta, B. Mery, C. Rodriguez-Lafrasse, N. Magne, *Med. Sci. Monit.* 2021, 27, 1–7.
- [9] X. Li, N. Kwon, T. Guo, Z. Liu, J. Yoon, *Angew. Chemie Int. Ed.* 2018, 57, 11522–11531.
- [10] E. L. Clennan, *Photochem. Photobiol.* 2022, 1–17.
- [11] J.-M. Aubry, C. Pierlot, J. Rigaudy, R. Schmidt, *Acc. Chem. Res.* 2003, 36, 668–675.
- [12] W. FUDICKAR, T. LINKER, in *PATAI'S Chem. Funct. Groups* (Ed.: L. John Wiley & Sons), John Wiley & Sons, Ltd, Chichester, UK, 2014, pp. 1–66.
- [13] W. Fudickar, T. Linker, *Angew. Chemie Int. Ed.* 2018, 57, 12971–12975.
- [14] W. Fudickar, T. Linker, *Chem. Commun.* 2008, 1771–1773.
- [15] W. Fudickar, T. Linker, *ChemPhotoChem* 2021, 5, 1004–1008.
- [16] M. Klaper, T. Linker, *Chem. - A Eur. J.* 2015, 21, 8569–8577.
- [17] W. Fudickar, T. Linker, *ChemPhotoChem* 2018, 2, 548–558.

- [18] Z. Gao, Y. Han, F. Wang, *Nat. Commun.* 2018, 9, 1–9.
- [19] D. Zehm, W. Fudickar, T. Linker, *Angew. Chemie - Int. Ed.* 2007, 46, 7689–7692.
- [20] P. De Bonfils, P. Nun, V. Coeffard, *European J. Org. Chem.* 2024, 202400099, DOI 10.1002/ejoc.202400099.
- [21] W. Fudickar, T. Linker, *Langmuir* 2010, 26, 4421–4428.
- [22] M. Agnes, A. Mazza, E. Kalydi, S. Béni, M. Malanga, I. Manet, *Chem. - A Eur. J.* 2023, 29, DOI 10.1002/chem.202300511.
- [23] S. Kolemen, T. Ozdemir, D. Lee, G. M. Kim, T. Karatas, J. Yoon, E. U. Akkaya, *Angew. Chemie Int. Ed.* 2016, 55, 3606–3610.
- [24] W. Fudickar, T. Linker, *Chem. - A Eur. J.* 2011, 17, 13661–13664.
- [25] W. Fudickar, T. Linker, *J. Am. Chem. Soc.* 2012, 134, 15071–15082.
- [26] R. H. YOUNG, R. L. MARTIN, D. FERIOZI, D. BREWER, R. KAYSER, *Photochem. Photobiol.* 1973, 17, 233–244.
- [27] I. B. C. Matheson, R. D. Etheridge, N. R. Kratowich, J. Lee, *Photochem. Photobiol.* 1975, 21, 165–171.
- [28] C. F. R. A. C. Lima, L. R. Gomes, L. M. N. B. F. Santos, J. N. Low, *Acta Crystallogr. Sect. E Struct. Reports Online* 2009, 65, o3037–o3037.
- [29] M. B. Plutschack, B. Pieber, K. Gilmore, P. H. Seeberger, *Chem. Rev.* 2017, 117, 11796–11893.
- [30] L. Capaldo, Z. Wen, T. Noël, *Chem. Sci.* 2023, 4230–4247.
- [31] M. S. Safiarian, A. Ugboya, I. Khan, K. O. Marichev, K. B. Grant, *Chem. Res. Toxicol.* 2023, 36, 1002–1020.